J. Fluid Mech. (2006), *vol.* 546, *pp.* 1–23. © 2005 Cambridge University Press
doi:10.1017/S0022112005006920 Printed in the United Kingdom

A continuum model of thermal transpiration

By JAMES R. BIELENBERG[1] AND HOWARD BRENNER[2]
[1]Los Alamos National Laboratory, ESA-MEE, Los Alamos NM 87545, USA
[2]Department of Chemical Engineering, Massachusetts Institute of Technology, Cambridge, MA 02139-4307, USA

(Received 25 January 2005 and in revised form 10 June 2005)

Previous proposed modifications in the respective constitutive forms of the Newtonian deviatoric stress tensor and the no-slip boundary condition imposed upon viscous fluids at solid surfaces, wherein the fluid's mass velocity is replaced by its volume velocity, furnishes a complete continuum-hydrodynamic description of thermal transpiration phenomena occurring in a closed capillary tube filled with a single-component gas or liquid, the former at negligibly small Knudsen numbers. The resulting expression for the steady-state thermomolecular pressure difference Δp existing between the two ends of the capillary, the latter maintained at different temperatures, is free of empirical parameters, such as Maxwell's thermal-slip coefficient, upon which current non-continuum theories of the phenomenon are based. The predicted Δp (with the pressure highest at the hotter end) is shown to agree well with experimental data for gases in the near-continuum limit of vanishingly small Knudsen number. Also discussed is the experimentally observed lack of dependence of Δp upon the physicochemical properties of the capillary walls, an observation which accords with the predictions of our theory. Our proposed volume velocity-based rationalization of the phenomenon of thermal transpiration offers a strictly continuum no-slip alternative to Maxwell's widely-accepted thermal creep explanation thereof, involving slip of the fluid's mass velocity at a non-isothermal surface. The agreement of our theoretical predictions of the thermomolecular pressure difference with experimental data, which is essentially indistinguishable in accuracy from that provided by Maxwell's thermal creep theory, provides further support for the viability of the generic volume velocity-based framework underlying our theory, the latter having recently been used to also rationalize related thermophoretic and diffusiophoretic phenomena in gases, as well as thermal diffusion in liquids.

1. Introduction

Consider the steady-state situation shown in figure 1 involving a closed-ended capillary tube with insulated sidewalls, filled with a single-component fluid (liquid or gas) whose hot and cold ends are maintained at uniform temperatures, T_+ and T_-, respectively. Gravity effects are supposed negligible. According to conventional hydrodynamic and transport processes notions, including the no-slip assumption on the bounding surfaces of the capillary tube, no fluid motion should exist in the capillary, with the only transport phenomenon taking place being that of steady-state one-dimensional axial heat conduction between the hot and cold ends of the tube. Concomitantly, owing to the absence of fluid motion, the pressure is predicted to be uniform throughout the tube, whence, the pressures, p_+ and p_-, at the respective hot and cold ends of the capillary tube would be expected to be equal. Explicitly, in the case

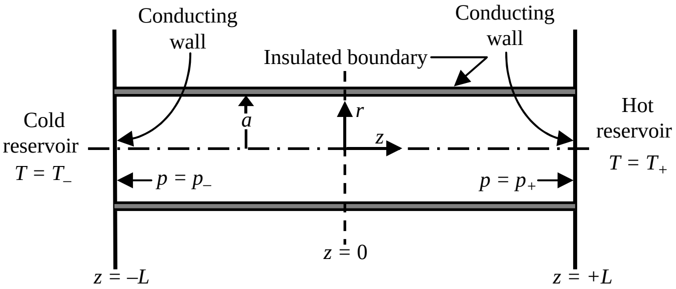

Figure 1. Thermal transpiration model system.

where the fluid's thermal conductivity is taken to be temperature independent, the only steady-state phenomena expected to occur are a linear diminution in temperature from T_+ to T_- along the length of the capillary, accompanied by a corresponding isobaric increase in the fluid's density, the latter as governed by the appropriate equation of state, $\rho = \rho(T)$, at the presumably uniform pressure, with $(\partial\rho/\partial T)_p < 0$. However, upon performing this experiment with a gas-filled capillary, Reynolds (1879) observed that, beginning with an initially uniform pressure in the originally isothermal gas, a steady-state pressure difference, $\Delta p = p_+ - p_- > 0$, eventually developed between the ends of the capillary following imposition of the temperature difference $\Delta T = T_+ - T_-$. (Reynolds' experiments were conducted with porous disks rather than actual capillary tubes, with the individual pores in the former case likened to single capillaries.) This thermomolecular pressure phenomenon, which has subsequently been confirmed by many others employing a host of different gases (e.g. Knudsen 1910; Los & Ferusson 1952; Annis 1972), is termed thermal transpiration. This terminology was originally coined by Reynolds (1879) in the course of his attempt to explain the workings of Crookes's radiometer (Crookes 1876), a 'toy' whose then mysterious windmill rotation when exposed to light or heat fascinated contemporary observers, including some of the outstanding scientists of the day (Brush 1976).

As is subsequently discussed, two rather different theories, both limited to gases, have since been advanced to explain the phenomenon of thermal transpiration in the so-called 'near-continuum' gas-kinetic theory limit of vanishingly small Knudsen numbers. Both theories, however, lie outside the respective realms of: (i) conventional continuum hydrodynamics and linear transport theory processes (Bird, Stewart & Lightfoot 2002), the latter being based upon classical irreversible thermodynamic principles (de Groot & Mazur 1984); and (ii) classical near-continuum first-order molecular theories (Hirschfelder, Curtiss & Bird 1954; Chapman & Cowling 1970). The older of the two theories, due to Maxwell (1879), derives from non-continuum arguments and supposes that the presence of molecular effects results in thermal 'slip' ('thermal creep') of the fluid's barycentric (or mass) velocity $\boldsymbol{v}_m$ along the surface of the capillary. (These non-continuum effects, which lie at the core of the two analyses cited, are invoked despite the fact that thermal transpiration is observed to occur under circumstances where the bulk fluid conditions lie well within the range normally encompassed by conventional continuum transport models (Bird *et al.* 2002), namely, where Knudsen numbers, $Kn = \lambda/a$, based upon the mean-free path λ and capillary tube radius a, are very much less than unity.) A second explanation, due to Derjaguin & Yalamov (1965, 1972), is based upon an approach which they refer to as constituting 'the kinetics and thermodynamics of stationary processes' (Derjaguin & Yalamov 1972). This scheme represents a combination of non-conventional irreversible thermodynamics (de Groot & Mazur 1984) and kinetic theory (Chapman & Cowling 1970), including second-order corrections to the heat flux associated with energy transport occurring in the non-continuum, so-called Knudsen layer proximate to solid surfaces.

In contrast with both Maxwell's (1879) molecularly-based theory and the seemingly *ad hoc* theory of Derjaguin & Yalamov (1972), we offer here an unconventional, but nevertheless purely macroscopic, continuum-hydrodynamic explanation of thermal transpiration, deriving from the disparity existing between the fluid's volume velocity field $\boldsymbol{v}_v$ and its mass-based barycentric velocity field $\boldsymbol{v}_m$ (Brenner 2004, 2005*a*, *b*). Our ability to provide a rational and straightforward, albeit unconventional, hydrodynamic explanation for thermomolecular pressure phenomena, free of molecularly based arguments, offers additional, albeit implicit, evidence (at least in the case of gases) of the reality of the velocity difference $\boldsymbol{v}_v - \boldsymbol{v}_m$ occurring in single-component fluids undergoing heat transfer, including the constitutive quantification of this velocity difference in terms of the diffuse flux density $\boldsymbol{j}_v$ of volume (Brenner 2005*a*) (see (10)–(11)).

2. Current understanding of thermal transpiration

2.1. *Maxwell's* (1879) *molecularly based interpretation of Reynolds'* (1879) *experiments*

In his widely cited work on thermal stresses arising in single-component thermally inhomogeneous gases, Maxwell (1879) derived the following result for the steady-state thermomolecular pressure difference occurring in a closed capillary tube:

$$p_+ - p_- = 8C_s \frac{\mu^2}{a^2 \rho T}(T_+ - T_-), \tag{1}$$

with μ, ρ and T, respectively, the fluid viscosity, density and absolute temperature. (Given the variation in temperature along the length of the capillary, the values of $\mu(T)$, $\rho(T)$ and T itself must be evaluated at some appropriate average value along the length of the capillary, thereby introducing some uncertainty into the precise pressure difference predicted by (1), an uncertainty which vanishes in the limit as the temperature difference between the ends goes to zero.) In this expression C_s is Maxwell's slip coefficient, a dimensionless $O(1)$ molecularly derived parameter, interpreted as being of non-continuum origin (Derjaguin *et al.* 1976; Talbot *et al.* 1980), and assumed generally to depend upon the composite physicochemical properties of the gas and capillary surface (Waldmann & Schmitt 1966). Maxwell's approximate calculation of this coefficient yielded $C_s = 3/4$, at least for Maxwell molecules (Chapman & Cowling 1970) upon supposing that these molecules are reflected diffusely from the wall.

Maxwell's (1879) result (presumably limited to monatomic gases according to his derivation thereof, although the noble, i.e. monatomic, gases were unknown in Maxwell's time) was originally given as

$$p_+ - p_- = 6 \frac{\mu^2}{a^2 \rho T(1 + G/a)}(T_+ - T_-),$$

with G a slip length,

$$G = \frac{2}{3}\left(\frac{2}{f} - 1\right)\lambda,$$

characterizing the purely hydrodynamic, isothermal mass velocity slip, arising from the non-continuum nature of a gas of otherwise uniform temperature and density in contact with a surface. (This G-based slip effect is different from Maxwell's thermal stress-induced slip, equation (2), since the former can exist even in isothermal systems.) Here, f is the fraction of incident molecules diffusively scattered at the wall ($0 < f < 1$). Upon substituting the expression for G into the general expression for Δp, it is apparent that the correction made by including the isothermal slip factor scales as $\lambda/a = Kn$. As such, its effect disappears as $Kn \to 0_+$. This is in contrast to the thermal slip portion of the tangential boundary condition on the barycentric velocity, which does not scale (directly) with the Knudsen number and, thus, does not vanish as the Knudsen number goes to zero (Kogan 1973, 1986, 2003; Kogan, Galkin & Friedlander 1976; Bobylev 1995; Alexandrov, Friedlander & Nikolsky 2003).

Maxwell derived (1) by solving the $\boldsymbol{v}_m$-based incompressible creeping flow equations (including the thermal stress enhancement thereof) and energy equations for the pressure difference arising from a zero net cross-sectional-mean mass flow condition within the capillary, acting in concert with the following thermal stress-induced generic slip boundary condition imposed upon the relative tangential component of the fluid's barycentric velocity along the surface ∂V_s of a solid boundary (the capillary sidewalls in the present case):

$$\boldsymbol{I}_s \cdot \boldsymbol{v}_m = C_s \frac{\mu}{\rho} \nabla_s \ln T \quad \text{on} \quad \partial V_s. \tag{2}$$

Here, $\boldsymbol{I}_s = \boldsymbol{I} - \boldsymbol{nn}$ is the surface projection operator in which $\boldsymbol{I}$ is the dyadic idemfactor, $\boldsymbol{n}$ a unit outer normal to the fluid on ∂V_s, and $\nabla_s = \boldsymbol{I}_s \cdot \nabla$ the surface gradient operator. Equation (2) embodies the notion, due to Maxwell (1879), that the existence of a temperature gradient ∇T in a gas along a solid surface gives rise to a thermal stress, stemming, in effect, from non-continuum Knudsen boundary-layer effects existing in the neighbourhood of the solid boundary; this, in turn, causes a local mass flow, $\boldsymbol{v}_m \neq \boldsymbol{0}$, to occur along ∂V_s, thus violating the classical no-slip tangential velocity boundary condition imposed upon $\boldsymbol{v}_m$ at solid surfaces.

2.2. *Review of experimental data*

As is evident from (1), an excess pressure exists at the hotter end of the capillary, even though no net cross-sectionally-averaged mass flow exists within the capillary. While this relation is found to accord moderately well with experiment, Derjaguin & Yalamov (1972) report that with use of Maxwell's original slip coefficient of $C_s = 3/4$, this equation underpredicts experimental results by a factor of approximately two (see the discussion of this factor following (49)). Their alternative theory (Derjaguin & Yalamov 1965) yielded the following expression for the thermomolecular pressure difference in gases:

$$p_+ - p_- = \frac{6\mu_o^2 R}{a^2 M(\omega + 1) p T^{2\omega+1}} \left(T_+^{2\omega+1} - T_-^{2\omega+1}\right), \tag{3}$$

with μ_o the viscosity at the reference temperature T_o, M the molecular weight, p the pressure within the system prior to the temperature difference being applied, T the arithmetic average of the two end temperatures, R the universal gas constant, and

ω a dimensionless constant, which, as a rule, is taken to be less than unity, being dependent upon the specific gas present in the system. Equation (3) for Δp was shown by Derjaguin & Yalamov (1972) to be in closer agreement with Knudsen's (1910) experiments on hydrogen at a mean pressure of 13 mm Hg, than that predicted by (1). Knudsen's additional experimental results for hydrogen at substantially lower mean pressures do not, however, agree nearly as well with (3), a difference attributed (Derjaguin & Yalamov 1965) to an additional non-continuum velocity slip at solid surfaces, over and above that due to Maxwell thermal slip, as earlier discussed.

Annis (1972) performed a series of experiments on various monatomic and polyatomic gases at Knudsen numbers much less than unity ($Kn \approx 10^{-2}$). In these experiments, a concentric tube arrangement was employed with a Pyrex capillary surrounded by a second nickel tube. The tubes were then connected to large nickel blocks maintained at specified temperatures. In this way, the imposed temperature gradient in the capillary could be held fixed to within 0.5 °K (approx. 0.2 % of the imposed temperature difference). Their experimental data were plotted on graphs of Δp *vs.* $1/p$, in accordance with the predictions of both (1) and (3) (cf. (50)). These data were fitted with a straight line (whose standard deviation for each gas tested ranged from 1.2 to 5.6 %). It was found that the measured thermomolecular pressure difference consistently fell somewhere between the predictions of (1) (where $C_s = 3/4$) and (3).

A set of experiments performed by Los & Fergusson (1952) preceding those of Annis (1972), and carried out using a similar scheme, measured the thermomolecular pressure difference existing in both argon- and nitrogen-filled capillaries. The temperature difference was controlled somewhat less rigorously, as it was imposed by holding one end of the sample cell in a Dewar flask containing a cryogenic liquid while the other was maintained at room temperature. The result of this was an imposed temperature gradient that could vary by as much as ∼1 %. They measured a correction to Maxwell's original estimate, $C_s = 0.75$, of the thermal slip coefficient, finding that for a given gas the measured correction factor, $\varpi := C_s/0.75$, to Maxwell's slip coefficient was independent of the capillary-wall material (nickel, Pyrex and glass tubing) and ranged from $\varpi = 1.35$ to 1.50. (These authors do not give explicit error estimates for the reported values of ϖ. However, the pressure drop data that were fitted to generate these values embodied disparities as large as 20 % for the higher-pressure measurements, the latter representing the range of greatest interest in connection with our current work.) Los & Fergusson's observation that the slip coefficient is independent of the physicochemical nature of the capillary-wall material appears especially surprising when we consider that Maxwell's slip (or comparable surface accommodation) arguments suggest that the gas–wall intermolecular interactions, dependent for a given gas upon the physicochemical wall properties (Sharipov 2004), should be of paramount importance in quantifying thermal transpiration. The importance of this observed property-independence in adding to the credibility of our subsequently proposed, purely hydrodynamic, theory of thermal transpiration is commented upon later.

Finally, a thermal transpiration study (Passian *et al.* 2003) was conducted using a micromechanical cantilever in order to probe the effects of mean pressure (and thus Knudsen number) on the resulting thermomolecular pressure difference (or what the investigators thereof refer to as the 'Knudsen force'). The latter experiments show that in the continuum and near-continuum limits (these being the limits of interest in the current work) the pressure difference (or equivalent Knudsen force) varies linearly with the inverse of the mean pressure. This result is consistent with the previous experimental studies noted above, which predict that Δp varies inversely with p.

In an effort to understand the molecular nature of thermomolecular pressure as well as the thermal mass slip underlying this phenomenon, Rosner and Papadopoulos (Rosner 1989; Papadopoulos & Rosner 1995; Rosner & Papadopoulos 1996) used molecular dynamics to simulate the flow induced in a closed container by an externally imposed temperature difference. Their results revealed the presence of 'convection-type rolls' even in the absence of gravity. The existence of such recirculating cells was rationalized by those authors as arising from a presumed mass slip occurring at the walls, similar to that expressed by (2), acting in concert with the absence of a net cross-sectionally-averaged mass flow.

While the respective non-continuum theories of Maxwell (1879) and Derjaguin & Yalamov (1965) accord reasonably well with experiments, both lack a truly theoretical justification given the essentially continuum state prevailing within the several gases investigated under the existing experimental conditions. This raises the issue of attempting to identify the subcontinuum source of the driving force(s) creating the recirculating flows observed by Papadopoulos and Rosner (Rosner 1989; Papadopoulos & Rosner 1995; Rosner & Papadopoulos 1996). More specifically, the question addressed is what is the nature of the molecular-scale physical phenomenon or phenomena, as revealed by their molecular-dynamics simulations, that serves to animate the flow along the walls associated with their observed internal recirculation? Furthermore, if surface–gas intermolecular interactions contribute to the magnitude of the thermomolecular pressure difference, why is this pressure difference found experimentally to be independent of the surface constitution of the capillary walls, as noted by Los & Fergusson (1952)?

2.3. *Review of our continuum hypothesis*

Subsequent sections propose a purely continuum-level explanation of the phenomenon of thermal transpiration, applicable in the case of gases to systems wherein the Knudsen number is effectively zero, and, hence, for which arguments of a strictly continuum nature should be applicable; that is, rather than invoking any non-continuum molecular or nonlinear arguments, such as those leading to (2) and therefore to (1), or, alternatively, introducing seemingly *ad hoc* irreversible thermodynamic arguments, such as those leading to (3), we instead employ an unconventional, albeit purely continuum-level, scheme (Brenner 2005*b*) to explain the phenomenon of thermal transpiration. The (generic) modified continuum equations and no-slip boundary condition underlying this scheme have previously been demonstrated to reproduce gaseous experimental thermophoretic (Brenner & Bielenberg 2005) and diffusiophoretic (Bielenberg & Brenner 2005*b*) data in the so-called 'near-continuum' (Chapman & Cowling 1970) regime prevailing at extremely small Knudsen numbers. (Moreover, these same arguments furnish results for thermal diffusion in liquids (Bielenberg & Brenner 2005*a*) that agree well with experimental data, although the evidence in that case is of a secondary rather than primary nature. Explicitly, the proposed scheme for explaining and quantifying thermomolecular pressure phenomena will be seen to be completely analogous to classic Poiseuille-type flow calculations for constant-density fluids, albeit adopting a constitutive relation for the deviatoric portion of Newton's rheological stress tensor based upon use of the fluid's volume velocity $\boldsymbol{v}_v$ (Brenner 2004, 2005*a*, *b*) in place of its mass or barycentric velocity $\boldsymbol{v}_m$, together with a comparable change in the choice of velocity upon which the no-slip boundary condition is to be imposed.

3. Steady-state flow in a closed capillary animated by a temperature difference imposed across its ends

3.1. *Basic equations*

Consider the case of a single-component fluid, liquid or gas, contained in the closed circular capillary tube (of large aspect ratio, $a/L \ll 1$) shown in figure 1, and obeying the single-component isobaric law of adiabatically additive volumes (Brenner 2005*a*), namely

$$\mathrm{d}\hat{v}/\mathrm{d}T = \text{const.} = K_v, \tag{4}$$

say, wherein

$$\hat{v} = 1/\rho \tag{5}$$

is the specific volume, and in which the constant K_v is independent of T. The complete set of gravity-free equations (Brenner 2004, 2005*b*) governing the steady-state transport of volume, momentum and energy occurring within the capillary are given, respectively, by the following trio of (dimensional) equations:

(i) Volume:

$$\nabla \cdot \boldsymbol{v}_v = 0; \tag{6}$$

(ii) Linear momentum:

$$\rho \boldsymbol{v}_m \cdot \nabla \boldsymbol{v}_m = -\nabla p + \mu_o \nabla^2 \boldsymbol{v}_v; \tag{7}$$

(iii) Energy:

$$\rho(\hat{c}_p)_o \boldsymbol{v}_m \cdot \nabla T = k_o \nabla^2 T + \nabla \cdot (p \boldsymbol{j}_v) + \beta T \, \boldsymbol{v}_m \cdot \nabla p + 2\mu_o (\nabla \boldsymbol{v}_v)^{sym} : (\nabla \boldsymbol{v}_m)^{sym}, \tag{8}$$

in which $\beta = -\rho^{-1}(\partial \rho/\partial T)_p \equiv K_v \rho$ is the fluid's coefficient of thermal expansion, and $\boldsymbol{D}^{sym} = (\boldsymbol{D} + \boldsymbol{D}^T)/2$ for any dyadic $\boldsymbol{D}$. Here, and throughout, the subscript 'o' affixed to a physical property that would ordinarily vary with temperature (and, hence, position) refers to some approximate average value of the physical property over the temperature range of interest; for example, $\mu_o = \mu(T_o)$, with T_o the average temperature at which the property is evaluated.

For simplicity, in the preceding transport equations, we have assumed the constancy of k and μ, as well as of the specific heat capacity $\hat{c}_p$, in addition to our prior assumption, (4), of adiabatically additive volumes. While the former assumptions are neither essential to the subsequent analysis nor entirely accurate when the temperature difference, $T_+ - T_-$, is large, they nevertheless enable us to focus attention on the essential physics of the problem without introducing distracting algebraic complications.

The usual mass-based continuity equation,

$$\nabla \cdot (\rho \boldsymbol{v}_m) = 0, \tag{9}$$

does not constitute an independent transport equation owing to the fundamental relation (Brenner 2005*a*),

$$\boldsymbol{v}_v = \boldsymbol{v}_m + \boldsymbol{j}_v, \tag{10}$$

in which the diffusive volume current is given constitutively by the expression (Brenner 2005*a*)

$$\boldsymbol{j}_v = -\frac{k_o}{(\hat{c}_p)_o} K_v \nabla T, \tag{11}$$

wherein pressure effects on the density of the fluid have been assumed small compared with those due to temperature effects.

3.2. *Boundary conditions*

As in figure 1, let (r, z) denote a symmetrical system of circular cylindrical coordinates, with $\hat{\boldsymbol{r}}$ and $\hat{\boldsymbol{z}}$ the corresponding unit vectors. In terms of these variables, the (dimensional) boundary conditions are:

(i) Temperature:

$$\hat{\boldsymbol{r}}\cdot\nabla T = 0 \quad \text{at } r = a \quad \forall(L > z > -L), \tag{12}$$

$$T = T_{\pm} \quad \text{at } z = \pm L \quad \forall(a > r > 0); \tag{13}$$

(ii) Velocity:

$$\hat{\boldsymbol{z}}\cdot\boldsymbol{v}_v = 0 \quad \text{at } r = a \quad \forall(L > z > -L), \tag{14}$$

$$\hat{\boldsymbol{r}}\cdot\boldsymbol{v}_m = 0 \quad \text{at } r = a \quad \forall(L > z > -L), \tag{15}$$

$$\hat{\boldsymbol{z}}\cdot\boldsymbol{v}_m = 0 \quad \text{at } z = \pm L \quad \forall(a > r > 0). \tag{16}$$

As regards the no-heat-flux boundary condition (12), in both Los & Fergusson's (1952) and Annis's (1972) experiments, discussed in § 1, the bounding walls of the capillary were not, in fact, insulated. Instead, measures were taken to ensure that a linear temperature gradient existed along the capillary sidewalls. Because of the large aspect ratio of the capillaries that we are considering, the governing equation for the temperature of the gas in the capillary reduces at leading order to a problem of pure heat conduction, resulting in a linear temperature gradient in the fluid, independent of radial position. This is what we subsequently find to be the case anyway (see (34)), even with use of the insulated capillary sidewall boundary condition, (12), at least insofar as the leading-order terms characterizing our solution scheme are concerned. Accordingly, in the interests of simplicity, we have chosen to regard the capillary as possessing insulated sidewalls for the purpose of comparing our theory with experiment. This enables attention to be focused exclusively on those transport processes occurring solely within the fluid, without having to deal simultaneously with the ensuing algebraic complications stemming from heat transfer through the solid phase surrounding the otherwise uninsulated capillary sidewalls.

3.3. *Non-dimensional scaling*

Define the following small dimensionless parameters:

$$\varepsilon = a/L \ll 1 \tag{17}$$

and

$$\gamma = \beta_o(T_+ - T_-) \ll 1, \tag{18}$$

where, as defined following (8), the subscript 'o' denotes some average temperature lying in the range between T_- and T_+, which will here be conveniently taken as $T_o = (T_+ + T_-)/2$. For reasons to be set forth subsequently, we also require satisfaction of the composite inequality,

$$\frac{\gamma}{\varepsilon} \ll 1, \quad \text{i.e.} \quad \gamma \ll \varepsilon \ll 1. \tag{19}$$

The following scaling applies, wherein a quantity to which an asterisk is affixed denotes a dimensionless scaled field or variable:

$$T = T_o(1 + \gamma T^*), \tag{20}$$

$$\rho = \frac{\rho_o}{1 + \beta_o(T - T_o)} \equiv \frac{\rho_o}{1 + \gamma\beta_o T_o T^*} \approx \rho_o(1 + \gamma\beta_o T_o T^*), \tag{21}$$

$$p = p_o + \gamma \frac{\mu_o \alpha_o}{a^2} p^*, \tag{22}$$

$$\boldsymbol{v} = \gamma \frac{\alpha_o}{L} (\hat{\boldsymbol{z}} v^* + \hat{\boldsymbol{r}} \varepsilon w^*). \tag{23}$$

In the above, $\alpha = k/\rho \hat{c}_p$ is the fluid's thermometric diffusivity. Quantities to which the subscript o is affixed are taken to be constants, evaluated at the reference temperature T_o. Equation (21) is equivalent to the adiabatic law of additive volumes, equation (4), since $\beta_o \equiv K_v \rho_o$. In the above, $\boldsymbol{v} = (\hat{\boldsymbol{z}} v + \hat{\boldsymbol{r}} w)$, with v and w, respectively, representing the radial and axial components of the dimensional vector velocity field $\boldsymbol{v}$. The velocity scaling embodied in (23) is the same for both $\boldsymbol{v} = \boldsymbol{v}_m$ and $\boldsymbol{v} = \boldsymbol{v}_v$. In view of (10), this same scaling necessarily applies to the axial and radial components of $\boldsymbol{j}_v$.

In addition to the preceding scalings of the various dependent-variable fields, we also have the following coordinate scalings for the independent variables:

$$z = L z^*, \quad r = a r^*, \tag{24}$$

whence

$$\nabla = \frac{1}{a}\left(\hat{\boldsymbol{r}} \frac{\partial}{\partial r^*} + \varepsilon \hat{\boldsymbol{z}} \frac{\partial}{\partial z^*}\right), \quad \nabla^2 = \frac{1}{a^2}\left[\frac{1}{r^*}\frac{\partial}{\partial r^*}\left(r^* \frac{\partial}{\partial r^*}\right) + \varepsilon^2 \frac{\partial^2}{\partial z^{*2}}\right]. \tag{25}$$

Each of the non-dimensional scaled fields appearing above, represented collectively by, say, the generic symbol $f^* = f^*(r^*, z^*; \gamma, \varepsilon)$, possesses the functional dependence indicated in the preceding argument of f^*. The scaling has been chosen such that in the limit where the two small parameters (17) and (18) each tend to zero, and in the 'outer' region, $1 > z^* > -1$ (i.e. not including the two 'inner' regions of dimensionless length $O(\varepsilon)$ existing in proximity to the two end caps, $z^* = \pm 1$), all of the outer fields are regular (i.e. non-singular) and hence of the form $f^*(r^*, z^*; \gamma, \varepsilon) = f^{*(0)}(r^*, z^*) + g^*(r^*, z^*; \gamma, \varepsilon)$, where the 'residue' g^* possesses the property that $\lim_{\varepsilon \to 0, \gamma \to 0} g^* = 0$. Thus, all of the outer fields to which the superscript (0) is affixed are dominant in the limit and each is a non-zero function, dependent, at most, only upon r^* and z^*.

4. Solution scheme

4.1. *Outer expansion*

Introduction of the preceding scaled variables into the transport equations (6)–(8), while retaining only those terms which dominate in the limit (17)–(19), yields the following quartet of scaled transport equations:

$$\frac{1}{r^*}\frac{\partial}{\partial r^*}\left(r^* w_v^{*(0)}\right) + \frac{\partial v_v^{*(0)}}{\partial z^*} = 0, \tag{26}$$

$$0 = -\frac{\partial p^{*(0)}}{\partial r^*} + \varepsilon \frac{1}{r^*}\frac{\partial}{\partial r^*}\left(r^* \frac{\partial w_v^{*(0)}}{\partial r^*}\right), \tag{27}$$

$$0 = -\frac{\partial p^{*(0)}}{\partial z^*} + \frac{1}{r^*}\frac{\partial}{\partial r^*}\left(r^* \frac{\partial v_v^{*(0)}}{\partial r^*}\right), \tag{28}$$

$$0 = \varepsilon^2 \frac{\partial^2 T^{*(0)}}{\partial z^{*2}} + \frac{1}{r^*}\frac{\partial}{\partial r^*}\left(r^* \frac{\partial T^{*(0)}}{\partial r^*}\right). \tag{29}$$

In the momentum and energy equations (27)–(29), we have recognized that terms of $O(\varepsilon^2)$ dominate over comparable terms of $O(\gamma^2)$ owing to the composite inequality

(19). As such, in deriving these equations, we have passed to the limit $\gamma \to 0$ while still retaining the more dominant terms in ε, namely those leading-order terms in ε which remain in the limit where $\varepsilon \ll 1$. It is this fact that has enabled us to neglect both the inertial terms in the momentum equation (7) compared with the viscous terms, and the convective and dissipative terms in the energy equation (8) compared with the conduction term. Upon passing to the second limit $\varepsilon \to 0$, it is seen that (27) separately requires that

$$\frac{\partial p^{*(0)}}{\partial r^*} = 0 \tag{30}$$

and

$$\frac{\partial}{\partial r^*}\left(r^*\frac{\partial w_v^{*(0)}}{\partial r^*}\right) = 0. \tag{31}$$

Likewise, (29) gives rise to the pair of equations,

$$\frac{\partial}{\partial r^*}\left(r^*\frac{\partial T^{*(0)}}{\partial r^*}\right) = 0 \tag{32}$$

and

$$\frac{\partial^2 T^{*(0)}}{\partial z^{*2}} = 0. \tag{33}$$

A first integration of (32) yields $r^*\partial T^{*(0)}/\partial r^* = F(z^*)$. A second integration thus gives $T^{*(0)} = F(z^*)\ln r^* + G(z^*)$, where F and G are integration functions to be determined. The requirement that the temperature be non-singular along the cylinder axis $r^* = 0$ requires that $F = 0$. Accordingly, $T^{*(0)}$ is, at most, a function only of z^*. As such, (33) reverts in status from a partial to an ordinary differential equation, $\mathrm{d}^2T^{*(0)}/\mathrm{d}z^{*2} = 0$, from which it follows that

$$\mathrm{d}T^{*(0)}/\mathrm{d}z^* = \text{const.} \tag{34}$$

Owing to the lack of dependence of $T^{*(0)}$ upon r^*, (34) automatically fulfils the boundary condition (12) expressing the fact that the cylinder sidewalls are insulated.

According to (30), $p^{*(0)}$ is independent of r^* and hence is, at most, a function only of z^*. Two consecutive integrations of (28) over r^* thus yields

$$v_v^{*(0)} = \frac{1}{4}\frac{\mathrm{d}p^{*(0)}}{\mathrm{d}z^*}r^{*2} + H(z^*)\ln r^* + I(z^*).$$

The requirement that $v_v^{*(0)}$ be non-singular along the axis of the capillary requires that $H = 0$. Furthermore, the no-slip volume velocity boundary condition, equation (14), requiring that $v_v^{*(0)} = 0$ at $r^* = 1$ for all $-1 < z^* < 1$ (possibly excluding the two end points $z^* = \pm 1$ belonging to the inner region) requires that $I = -(1/4)(\mathrm{d}p^{*(0)}/\mathrm{d}z^*)$. Consequently,

$$v_v^{*(0)} = \frac{1}{4}\frac{\mathrm{d}p^{*(0)}}{\mathrm{d}z^*}(r^{*2} - 1). \tag{35}$$

It remains yet, among other things, to determine the pressure gradient $\mathrm{d}p^{*(0)}/\mathrm{d}z^*$, which at this stage of the analysis is not necessarily a constant, but may depend upon z^*.

Owing to the boundary condition (12), equation (11) requires that $\hat{\boldsymbol{r}} \cdot \boldsymbol{j}_v = 0$ at $r = a$. Consequently, (10) in conjunction with the boundary condition (15) requires that $\hat{\boldsymbol{r}}\cdot\boldsymbol{v}_v=0$ at $r=a$. Expressed in scaled form, this requires that

$$w_v^{*(0)}=0 \quad \text{at } r^*=1. \tag{36}$$

A two-fold integration of (31), similar to that of our previous integration of (32), gives $w_v^{*(0)}=J(z^*)\ln r^* + K(z^*)$. The requirement that $w_v^{*(0)}$ be non-singular along the cylinder axis necessitates that $J=0$. In addition, the boundary condition (36), applicable for all z^* (in the outer region), further requires that $K=0$. Consequently,

$$w_v^{*(0)} = 0. \tag{37}$$

Substitution of (33) into (26) shows that $\partial v_v^{*(0)}/\partial z^*=0$. In turn, it thus follows from (31) that $\mathrm{d}^2p^{*(0)}/\mathrm{d}z^{*2}=0$. Consequently,

$$\frac{\mathrm{d}p^{*(0)}}{\mathrm{d}z^*} = \text{const}, \tag{38}$$

independent of z^*. All boundary conditions and transport equations have now been satisfied (to leading order) except for the ‘inner’ boundary conditions (13) and (16) prevailing at the ends of the capillary. Satisfaction of these will be seen to determine uniquely the values of the two unknown constants appearing in (34) and (38).

The mass-based continuity equation (9) together with the mass-based impenetrability conditions (15) and (16) leads straightforwardly to the conclusion that the total mass flux through any cross-sectional plane, $z=\text{const}$, in the capillary is necessarily zero. Explicitly, this requires that in the outer region,

$$\int_{r=0}^{a} \rho^{(0)} v_m^{(0)}\,\mathrm{d}A = 0, \tag{39}$$

where $\mathrm{d}A = 2\pi r\,\mathrm{d}r$ is an element of cross-sectional area. (This vanishing integral cross-sectional flow condition, which derives from the impermeability condition (16) imposed at the capillary ends in conjunction with (15), is an exact relation. As such, it applies in both the outer and inner regions.) Since the density is assumed to be a function only of temperature, and since the temperature $T^{(0)}$ is a function only of z, it follows that $\rho^{(0)}=\rho^{(0)}(z)$. As such, $\rho^{(0)}$ may be removed from beneath the integral sign, leading to the simpler requirement that $\int_{r=0}^{a} v_m^{(0)}\,\mathrm{d}A=0$. Since, from (10), $v_m=v_v-j_v$, the vanishing net mass flux requirement in the outer region is seen to be equivalent to the equality

$$\int_{r=0}^{a} v_v^{(0)}\,\mathrm{d}A = \int_{r=0}^{a} j_v^{(0)}\,\mathrm{d}A. \tag{40}$$

In dimensional form, (35) becomes

$$v_v^{(0)}=\frac{a^2}{4\mu_o}\frac{\mathrm{d}p^{(0)}}{\mathrm{d}z}\left[\left(\frac{r}{a}\right)^2-1\right]. \tag{41}$$

On the other hand, (11) is equivalent to

$$j_v^{(0)}=-\alpha_o\beta_o\frac{\mathrm{d}T^{(0)}}{\mathrm{d}z}. \tag{42}$$

Effecting the requisite integrations in (40) over r thus yields the following relation between the respective pressure and the temperature gradients:

$$\frac{\mathrm{d}p^{(0)}}{\mathrm{d}z} = \frac{8\mu_o\alpha_o\beta_o}{a^2}\frac{\mathrm{d}T^{(0)}}{\mathrm{d}z}. \tag{43}$$

Recall from (34) and (38) that both the outer pressure and temperature gradients appearing in the above equation are constants, independent of axial position z within the capillary.

4.2. *Inner expansion*

The equations derived thus far are strictly applicable only in the outer region, which excludes the end-cap cylindrical regions of lengths $O(a)$ lying near the respective ends, $z=+L$ and $z=-L$, of the capillary. Formally, analysis of the precise details occurring in these regions could be effected by defining the pair of 'inner' independent scaled variables, $\tilde{z}^*_+ = (1-z^*)/\varepsilon$ and $\tilde{z}^*_- = (1+z^*)/\varepsilon$, in the respective neighbourhoods of $z^*=+1$ and $z^*=-1$, thus rendering both $\tilde{z}^*_\pm = O(1)$ in the respective inner regions. In turn, in the language of matched asymptotic expansions of singular perturbation theory (Van Dyke 1975), the resulting inner fields must be matched with their outer field counterparts (in their common overlapping domains of validity). The outer fields have already been calculated above, modulo knowledge of the as yet unknown constants, $\mathrm{d}T^{(0)}/\mathrm{d}z$ and $\mathrm{d}p^{(0)}/\mathrm{d}z$, appearing therein. As such, the requisite matching scheme serves to determine uniquely, *inter alia*, the values of these two constants. It is in the neighbourhood of the two inner regions that the mass fluid motion, $\boldsymbol{v}_m$ (which will subsequently be seen to be flowing in the region proximate to the sidewalls from the hot towards the cold end of the capillary), must reverse direction as it encounters the end caps, in order that there be no net mass flow. Clearly, the detailed flow reversal occurring in these regions will lead to a quite complex mass velocity field, say $\tilde{\boldsymbol{v}}^{(0)}_m$, in the inner regions, possessing both axial and radial components. However, it is equally apparent that, despite this complexity, the respective temperatures in these regions will not depart sensibly from the values prescribed at the ends in (13). As such, it is obvious from the dimensional form of (34), together with the fact that this temperature gradient is uniform throughout the entire outer field of length $2L$, that a formal matching of the respective inner and outer temperature fields, $\tilde{T}^{(0)}$ and $T^{(0)}$ (with $\tilde{T}^{(0)}$ satisfying the inner boundary conditions (13)) will give rise to the following expression for the uniform temperature gradient in the outer region:

$$\frac{\mathrm{d}T^{(0)}}{\mathrm{d}z} = \frac{T_+ - T_-}{2L}. \tag{44}$$

The latter in conjunction with the constancy of $\mathrm{d}p^{(0)}/\mathrm{d}z$ throughout the outer region, jointly with (38), thus results in the following expression for the thermomolecuular pressure difference across the capillary:

$$p_+ - p_- = \frac{8\mu_o\alpha_o\beta_o(T_+ - T_-)}{a^2} \equiv \gamma\frac{8\mu_o\alpha_o}{a^2}, \tag{45}$$

this result for Δp being correct to terms of leading order in the small parameter γ. As such, according to our theory, provided that the fluid expands upon being heated, so that $\beta_o > 0$, find that $p_+ > p_-$, corresponding to the fact that the pressure will be highest at the hotter side of the capillary. Equation (45) is presumably equally applicable to both liquids and gases given the fact that our derivation does not, thus far, distinguish between these two states of matter. In view of the requisite inequality, $\gamma \ll 1$, it might appear that this pressure difference is necessarily small, and hence likely to prove difficult to observe experimentally, especially in liquids. (Of course, in the case of gases, Δp has already been successfully observed experimentally long ago by Reynolds (1879), despite the relative crudity of the equipment available to him at that time.) However, the magnitudes of the other physical parameters appearing in

(45) may be such that the resulting pressure difference is, in fact, quite large despite the smallness of γ. This situation could occur, for example, in the case of liquids of large viscosity or in capillaries of small radius. There is, of course, no restriction imposed upon the pressure difference Δp itself; rather, the only pressure-related requirement is that the effect of the local pressure gradient upon the density of the fluid be small compared with the corresponding effect thereon of the temperature gradient.

Although not explicitly required, in the interests of completeness, we note that when expressed in terms of the originally prescribed data, the respective volume- and mass-velocity fields in the outer region are, respectively,

$$\boldsymbol{v}_v^{(0)} = -\hat{\boldsymbol{z}}\gamma \frac{\alpha_o}{L}\left[1 - \left(\frac{r}{a}\right)^2\right], \tag{46}$$

$$\boldsymbol{v}_m^{(0)} = -\hat{\boldsymbol{z}}\gamma \frac{1}{2}\frac{\alpha_o}{L}\left[1 - 2\left(\frac{r}{a}\right)^2\right], \tag{47}$$

where the unit vector $\hat{\mathbf{z}}$, which points in the direction of the temperature gradient (figure 1), is directed from the cold towards the hot end of the capillary. Upon setting $r = a$ in (47), it follows that $\hat{\boldsymbol{z}} \cdot \boldsymbol{v}_m \neq 0$ along the capillary sidewall, showing that $\boldsymbol{v}_m$ slips along this wall, just as in the case of Maxwell's thermal slip formula, (2). Accompanying this slip, we see that throughout the annular region, $a/\sqrt{2} < r \leqslant a$, proximate to the capillary wall, the fluid mass flows from cold to hot, while in the central core, $a/\sqrt{2} > r > 0$, the fluid mass reverses direction upon encountering the impermeable end caps, such that no net mass flow occurs in any capillary cross-section.

5. Detailed comparison with experiments

5.1. *The case of gases*

In the case of ideal gases, we have $\beta = 1/T$. Moreover, the Prandtl number is defined as $Pr = \upsilon/\alpha$, where $\upsilon = \mu/\rho$ is the kinematic viscosity. Accordingly, upon suppressing the arbitrary reference affix o in (45) we obtain

$$p_+ - p_- = 8C_s' \frac{\mu^2}{a^2 \rho T}(T_+ - T_-), \tag{48}$$

where $C_s' = 1/Pr$. (The coefficient C_s' appearing in (48) is the exact counterpart of Maxwell's mass-velocity slip coefficient C_s in (2) for the barycentric slip velocity, in the sense that in present circumstances we have from (47) and (44) that $\hat{\boldsymbol{z}}\hat{\boldsymbol{z}} \cdot \boldsymbol{v}_m^{(0)} = \alpha_o \hat{\boldsymbol{z}}\, \mathrm{d}T^{(0)}/\mathrm{d}z$ at $r = a$, wherein $\alpha_o = C_s' \upsilon_o$ by the definition that $C_s' = 1/Pr$.) Except for the possible difference in slip coefficients between our C_s' and Maxwell's C_s in (1), the two formulae are constitutively identical, despite their having been obtained by very different arguments. According to the Eucken relation (Bird *et al.* 2002), $Pr = 2/3$ and $14/19$, respectively, for monatomic and diatomic gases. Consequently,

$$C_s' = (1.5, 1.36) \quad \text{(monatomic, diatomic)}. \tag{49}$$

In the case of monatomic gases, our slip coefficient, $C_s' = 3/2$, differs from Maxwell's $C_s = 3/4$ value by a factor of two. Recall, however, that Derjaguin & Yalamov (1965, 1972) claim that Maxwell's thermal transpiration formula, (1), in which $C_s = 3/4$, is too small by a factor of about two with regard to its agreement with experiment.

In the context of the penultimate sentence of the preceding paragraph, it is pertinent to note that Sharipov (2004) points out that according to kinetic theory, Maxwell's thermal slip coefficient C_s for monatomic gases may actually vary between 3/4 and

Gas	$d(\Delta p)/d(1/p)$ Experimental	Present work Equation (50)	Maxwell Equation (1)	Derjaguin & Yalmanov Equation (3)
Helium	4.4	6.7 (3.3–11.6)	3.3	7.0
Neon	2.0	3.7 (2.3–5.9)	1.8	3.5
Argon	0.63	1.1 (0.6–1.8)	0.5	1.0
Krypton	0.46	0.7 (0.4–1.2)	0.3	0.7
Nitrogen	0.50	0.9 (0.5–1.4)	0.4	0.8

TABLE 1. Comparison of the experimental results of Annis (1972) with the three thermal transpiration theories. All tabular values above are reported in pressure-squared units of $(\text{torr})^2$. Experimental parameter values used in (50) were evaluated at the arithmetic mean temperature, $(T_+ + T_-)/2$, of the ends of the capillary. Limiting property values, based upon evaluating physical properties at the extreme temperature limits, T_+ and T_-, respectively, rather than at the mean temperature, and presumably bracketing the range of possible values predicted by the present theory, are reported parenthetically in the column labeled 'Present work'. That the above results for the four rare gases are not exactly twice of those Maxwell's is due simply to our having rounded out the first decimal place in the tabulation so as to properly reflect the uncertainty in the experimental data relative to the estimated degree of approximation implicit in our theoretical calculations by virtue of our having replaced temperature-dependent gas properties such as viscosity by average position-independent values thereof. In making the comparable comparison with Maxwell's theory in the case of the nitrogen, it should be borne in mind that nitrogen is a diatomic gas, whose specific heat ratio is different from that for Maxwell's monatomic 'Maxwellian' molecules (cf. (49)).

3/2, where the first value corresponds to the diffuse reflection of molecules from the surface (the model originally adopted by Maxwell (1879) based upon his implicit, albeit somewhat arbitrary, choice of an accommodation coefficient), while the second value corresponds to the opposite situation, namely back reflection. The second value cited by Sharipov (2004), namely $C_s = 3/2$, accords exactly with our result for the slip coefficient, derived from our strictly continuum-level assumption that there is no slip of the volume velocity at a solid surface (combined with use of the ideal-gas specific heat ratio, $\hat{c}_p/\hat{c}_v = 5/3$, for monatomic gases). As such, the factor of two distinguishing our prediction of the thermomolecular pressure Δp for the case of monatomic gases from that of Maxwell, (1), can be rationalized in terms of differing molecular-level assumptions about the magnitude of the accommodation coefficient at a solid surface.

5.2. *Comparison of the several theoretical models with experiments performed on gases*

Below, we compare our thermomolecular pressure prediction, (48), as well as those of previous investigators, namely (1) and (3), with Annis's (1972) experimental observations on gases. To do so, we recast (48) into a more appropriate form by supposing ideal gas behaviour, namely $\rho T = (M/R)p$, appropriate to Annis's experiment. This results in the expression

$$p_+ - p_- = C_s' \left[\frac{8\mu^2 R(T_+ - T_-)}{a^2 M}\right] \frac{1}{p}. \tag{50}$$

Table 1 shows the requisite comparison. (The theoretical comparisons presented by Annis (1972) appear in graphical, rather than tabular numerical, format. As such, small errors may have been incurred during our estimation from those graphs of the numerical values displayed in table 1.) Annis's (1972) experiments were performed at very small Knudsen numbers ($Kn \approx 10^{-2}$), spanning multiple mean pressure values for the five different gases studied (both monatomic and diatomic). He observed that a plot of the experimental data in the form of Δp *vs.* $1/p$ for a given gas–capillary system yielded a straight line (standard deviation from a linear fit for each gas tested ranged from 1.2 to 5.6 %), bearing in mind that the viscosity of an ideal gas is independent of pressure (Bird *et al.* 2002, p. 21). This $1/p$ dependence of the thermomolecular pressure difference also accords with the experimental work of Passian *et al.* (2003). As such, comparison of Annis's experimental measurements with the respective theoretical predictions of the resulting slope, $\mathrm{d}(\Delta p)/\mathrm{d}(1/p)$, provides an effective measure of the accuracy of each of the three theories.

Table 1 shows all three theoretical approaches to be consistent with the experimental data of Annis. It is important to recall, however, that the theories of Maxwell (1879) and Derjaguin & Yalmanov (1965) employed molecularly based arguments and semi-empirical parameters of perhaps questionable validity to predict the effective barycentric velocity slip at the capillary wall surface. Moreover, each entailed a second shear-slip parameter (see the paragraph following (1)), requiring knowledge of the wall's accommodation coefficient, an empirical parameter, for the particular gas confined within. In contrast, the purely continuum hydrodynamic theory used in our work is devoid of any such adjustable parameters.

Our generic volume–velocity-based no-slip boundary condition renders the pressure drop expression, (50), independent of the material properties of the capillary walls (such independence being similar to what has always been observed to be the case for conventional isothermal single-component flow results derived using the classical no-slip boundary condition imposed upon $\boldsymbol{v}_m$). As such, our predictions are consistent with the results of Los & Fergusson (1952), who demonstrated that the thermomolecular pressure drop was the same for all of the materials studied by them (Pyrex, glass and nickel). Qualitatively, the predictions for the experimental pressure drop derived in this work are somewhat higher than those presented by the preceding authors, with our theory predicting the following slip-coefficient corrections due to Los & Fergusson (1952): $\varpi_{\mathrm{Argon}} = 2$ (*vs.* the measured values $\varpi_{\mathrm{Argon}} = 1.35 - 1.5$) and $\varpi_{\mathrm{Nitrogen}} = 1.8$ (*vs.* the measured value of $\varpi_{\mathrm{Nitrogen}} = 1.35$). It appears that, even to within the reported and/or expected experimental error, the predictions of our theory are systematically somewhat high. It is not clear if this disparity is due to the various approximations made during the course of the calculations (e.g. temperature-independence of viscosity, thermal conductivity, etc.) or to a more fundamental source.

In our search of the thermal transpiration literature, we were unable to find any experimental studies of thermomolecular pressure in liquids. However, in anticipation of future experiments, (45) allows us to make order-of-magnitude predictions about such effects, useful in designing appropriate experiments. For, say, toluene, this would result in $\Delta p/\Delta T \approx 1 \times 10^{-4}$ Pascal/Kelvin in a channel with a 50 μm radius, or $\Delta p/\Delta T = O(1)$ Pascal/Kelvin for a channel with a radius of the order of 1 μm. Obviously, if our theory is correct, the choice of a fluid of much higher viscosity than that of toluene would render the requisite measurements more experimentally accessible. At first glance, the characteristic channel dimensions given above may seem small. However, given current manufacturing techniques in the field of microfluidics, such experiments appear to lie with the realm of possibility (Passian *et al.* 2003).

6. Discussion and conclusions

6.1. *Force balance*

Beyond the observed accord with experiment discussed in the previous section, the thermal transpiration results presented herein appear to be dynamically consistent, albeit requiring recognition that systems which are closed to net mass flow may, nevertheless, be open to volume 'flow' in a dynamical sense (Brenner 2005*a*). For example, since no external force acts on the fluid contained in the capillary, and since the motion is steady, it is not inappropriate to wonder what force serves to balance the pressure force $A\Delta p$ (with $A = \pi a^2$ the cross-sectional area of the capillary) acting over the ends owing to the existence of the thermomolecular pressure difference, Δp. In our treatment, it is evident that this balancing force must stem from the viscous stresses acting along the walls of the capillary as a consequence of the axial non-zero volume velocity shear rate, $\partial v_v^{(0)}/\partial r$ at $r = a$. This is readily confirmed because in the absence of inertial effects, to which to our zero-order approximation (27)–(28) conforms, the pressure tensor is solenoidal,$\nabla \boldsymbol{\cdot} \boldsymbol{P}_v^0 = \boldsymbol{0}$, wherein $\boldsymbol{P}_v^{(0)} = -\boldsymbol{I}p^{(0)} + \boldsymbol{T}_v^{(0)}$, with the deviatoric portion $\boldsymbol{T}_v^{(0)}$ of this stress based upon Newton's law of viscosity, in which $\boldsymbol{v}_v$ appears in place of $\boldsymbol{v}_m$ (Brenner 2004, 2005*b*). As such, the net external force, $\boldsymbol{F}^{(0)} = \oint_{\partial V} \mathrm{d}\boldsymbol{S} \boldsymbol{\cdot} \boldsymbol{P}_v^0$, exerted by the surroundings on the fluid contained within the capillary must be identically zero, requiring that the pressure force $A\Delta p$ acting over the ends of the capillary exactly balance the shearing force along the walls. That is, with $\boldsymbol{F}^{(0)} = \boldsymbol{F}_{\pm}^{(0)} + \boldsymbol{F}_w^{(0)} = \boldsymbol{0}$, in which the symbols have an obvious meaning, it follows that $\boldsymbol{F}_w^{(0)} = -\boldsymbol{F}_{\pm}^{(0)}$. This leads to the conclusion that the external force exerted by the surroundings on the wall is

$$\boldsymbol{F}_w^{(0)} = \hat{\boldsymbol{z}}\pi a^2 \left(p_+^{(0)} - p_+^{(0)}\right), \tag{51}$$

a result which we have confirmed by direct integration of the stresses, $\boldsymbol{F}_w^{(0)} = \oint_{\partial V_s} \mathrm{d}\boldsymbol{S} \boldsymbol{\cdot} \boldsymbol{P}_v^0$, acting over the sidewalls ∂V_s of the capillary.

6.2. *Thermodynamic considerations*

Interesting and fundamental issues arise with respect to thermodynamic considerations of energy conservation and entropy production in regard to the intrinsic differences between Maxwell's (1879) theory of thermal transpiration and our theory, as herein outlined. However, these disparities are not resolvable at the present zero-level of approximation, but rather require explicitly addressing the higher-order terms in our perturbation scheme, currently unavailable. Indeed, calculation of the higher-order terms in the expansion would also be of interest in terms of establishing whether or not this would improve the agreement of the present theory with Annis's (1972) and Los & Fergusson's (1952) experiments.

6.3. *The physical basis for regarding* $\boldsymbol{v}_v$ *rather than* $\boldsymbol{v}_m$ *as the fluid velocity* $\boldsymbol{v}$

The present study was motivated solely by the desire to provide further experimental support for the credibility of our modified theory of viscous fluid mechanics (Brenner 2004, 2005*b*), above and beyond the experimental evidence already offered in this connection with regard to the phenomena of thermophoresis (Brenner & Bielenberg 2005) and diffusiophoresis (Bielenberg & Brenner 2005*b*) in the case of gases, and thermal diffusion (Bielenberg & Brenner 2005*a*) in the case of liquids. When comparing theory with experiment, it is important to note that $\boldsymbol{v}_m = \boldsymbol{v}_v$ identically in the case of so-called 'incompressible' fluids (Brenner 2005*a*), namely fluids whose density ρ is uniform throughout. As such, the huge body of data already available for incompressible fluid experiments, currently serving to support Stokes' original $\boldsymbol{v} = \boldsymbol{v}_m$-based no-slip hypothesis, $\boldsymbol{I}_s \boldsymbol{\cdot} \boldsymbol{v}_m = \boldsymbol{0}$ (Lauga, Brenner & Stone 2005), as well as Newton's rheological hypothesis, $\boldsymbol{T} = 2\mu\overline{\nabla \boldsymbol{v}_m} + \boldsymbol{I}\kappa\nabla \boldsymbol{\cdot} \boldsymbol{v}_m$ (where $\overline{\nabla \boldsymbol{v}}$ denotes the symmetric traceless velocity gradient dyadic and κ the dilatational or bulk viscosity), now also serve, with equal merit, to support both our $\boldsymbol{v} = \boldsymbol{v}_v$-based no-slip, $\boldsymbol{I}_s \boldsymbol{\cdot} \boldsymbol{v}_v = \boldsymbol{0}$, and Newton's law, $\boldsymbol{T} = 2\mu\overline{\nabla \boldsymbol{v}_v} + \boldsymbol{I}\kappa\nabla\cdot\boldsymbol{v}_v$, hypotheses. Note that the latter bulk viscosity contribution vanishes in circumstances where the law of additive volumes, (6), holds.

While agreement with experiment is the ultimate arbiter of the success of any theory, it is equally important to understand the theory's physical basis, especially when the theory purports to overthrow long-held physical notions about the phenomenon. Accordingly, in this subsection we summarize the underlying rationale behind the two proposed changes, namely from $\boldsymbol{v}_m$ to $\boldsymbol{v}_v$, of the velocity $\boldsymbol{v}$ appearing in the no-slip boundary condition, $\boldsymbol{I}_s\cdot\boldsymbol{v} = \boldsymbol{0}$ on solid surfaces, and in Newton's rheological constitutive law, $\boldsymbol{T} = 2\mu\overline{\nabla \boldsymbol{v}} + \boldsymbol{I}\kappa\nabla\cdot\boldsymbol{v}$, for the deviatoric stress. This rationale, which has not previously been fully articulated elsewhere, naturally predates its eventual application towards explaining any of the specific thermophoretic (Brenner & Bielenberg 2005), thermal diffusion (Bielenberg & Brenner 2005*a*), or diffusiophoretic (Bielenberg & Brenner (2005*b*) boundary-value problems that were solved during the course of attempting to verify the theory, including the present $\boldsymbol{v}_v$-based explanation of thermal transpiration phenomena.

The single physical principle underlying the proposed changes from $\boldsymbol{v}_m$ to $\boldsymbol{v}_v$ resides in the view (Brenner 2005*b*) that the velocity $\boldsymbol{v}$ appearing in the basic equations of continuum fluid mechanics should, physically, represent the Lagrangian velocity $\boldsymbol{v}_l$ of the fluid, the latter as defined by the expression $\boldsymbol{v}_l := (\partial \boldsymbol{x}/\partial t)_{\boldsymbol{x}_0}$. Here, $\boldsymbol{x} = \boldsymbol{x}(\boldsymbol{x}_0, t)$ denotes the instantaneous position in space at time t of the particular 'tracer' particle that at time $t = 0$ occupied the spatial position $\boldsymbol{x}_0$. The mapping $\boldsymbol{x} = \boldsymbol{x}(\boldsymbol{x}_0, t)$ corresponds to the spatio-temporal trajectory of the effectively point-size tracer particle bearing the identifying 'label' $\boldsymbol{x}_0$. Given the view that $\boldsymbol{v}_l$ represents the local physical velocity with which the fluid continuum moves through space (rather than, say, the statistically-mean velocity of a collection of mobile molecules as embodied in the notion of a so-called differentially-sized 'material fluid particle'), it appears natural to expect $\boldsymbol{v}_l$ to constitute the velocity $\boldsymbol{v}$ appearing, *inter alia*, in both Newton's law of viscosity and in the no-slip boundary condition. (Recall that a material fluid particle (MFP), is defined as being a body of fluid defined by the property that all of the points $\boldsymbol{x}$ lying on its surface move instantaneously with the local mass velocity $\boldsymbol{v}_m(\boldsymbol{x}, t)$ of the fluid, with the latter being the velocity appearing in the continuity equation (Slattery 1972). According to the Reynolds transport theorem, a material fluid particle always consists of the same amount of mass. However, the collective mass of molecules composing an MFP does not permanently consist of the same matter, since individual molecules are free to enter and leave the body through its intrinsically permeable surface. When effectively differential in size, an MFP is envisaged in the continuum fluid-mechanical literature (Slattery 1972) as constituting the 'tracer particle' being monitored when applying the definition of the fluid's Lagrangian velocity $\boldsymbol{v}_l$. However, lacking the permanence of a material entity, an MFP, being intrinsically ephemeral, cannot, experimentally, be monitored when applying the definition of $\boldsymbol{v}_l$ to an unchanging entity permanently identified by the label $\boldsymbol{x}_0$. Only an actual physical particle of unimpeachable integrity, one whose mass and matter coincide for all time, can serve this purpose.)

To the extent that $\boldsymbol{v}_l$ is thus regarded as being synonymous with the fluid's mass velocity $\boldsymbol{v}_m$ – the latter being the normalized flux density appearing in the continuity equation, $\partial\rho/\partial t + \nabla\cdot\boldsymbol{n}_m = 0$ (with $\boldsymbol{n}_m = \rho\boldsymbol{v}_m$ the flux density of mass) – it is entirely appropriate that the unadorned velocity symbol $\boldsymbol{v}$ appearing in both Newton's law of viscosity and the no-slip boundary condition should implicitly refer to the fluid's mass velocity $\boldsymbol{v}_m$. On the other hand, were it to be convincingly demonstrated by performing tracer experiments that $\boldsymbol{v}_l = \boldsymbol{v}_v$ – without invoking, *a priori*, the pair of

$\boldsymbol{v}_m \rightarrow \boldsymbol{v}_v$ changes that we have advocated – it would then be equally appropriate to identify the unadorned velocity $\boldsymbol{v}$ appearing in both Newton's law of viscosity and the no-slip condition with $\boldsymbol{v}_v$ when solving viscous boundary-value problems of the types being addressed in this and related papers (Brenner & Bielenberg 2005; Bielenberg & Brenner 2005*a*, *b*). From this objective perspective, the issue of which velocity, $\boldsymbol{v}_m$ or $\boldsymbol{v}_v$, if indeed either, is most likely to be the correct velocity $\boldsymbol{v} \equiv \boldsymbol{v}_l$ appearing in the dynamical equations of motion when solving viscous fluid boundary-value problems involving solid surfaces has to be based solely on the outcome of experiments performed wherein no macroscopic solid surfaces are present in the fluid, and in whose objective interpretation the issue of Newton's viscosity law is never invoked. We refer here to purely kinematical experiments, requiring knowledge neither of the correct dynamics nor energetics when interpreting the outcome of measurements of the fluid's velocity $\boldsymbol{v}$. Thus, for example, Bird *et al.* (2002, p. 534) posit 'that $\rho\boldsymbol{v}$ is the local rate at which mass passes through a unit cross section placed perpendicular to the velocity $\boldsymbol{v}$', stating further that: 'This is the local velocity one could measure by means of a Pitot tube..., and corresponds to the $\boldsymbol{v}$ used in the equation of motion and in the energy equation..., for pure fluids.' However, their scheme does not pose an objective measurement of $\boldsymbol{v}$, since the interpretation of the kinematical symbol $\boldsymbol{v}$ obtained in this manner hinges on the use of the so-called Bernoulli equation, a dynamical relation.

Our purely kinematical interpretation of experimental thermophoretic particle movement through gases (Brenner 2004, 2005*b*; Brenner & Bielenberg 2005) appears to confirm the view that Lagrangian velocity $\boldsymbol{v}_l$ of the fluid, as measured by monitoring the velocity of a physical 'tracer' particle as the latter pursues its trajectory through space, is not generally synonymous with $\boldsymbol{v}_m$, but rather with the fluid's volume velocity $\boldsymbol{v}_v$ (Brenner 2005*a*). As summarized in what follows, the argument underlying the belief that $\boldsymbol{v}_l = \boldsymbol{v}_v$ is based upon a straightforward purely kinematical calculation of the volume velocity $\boldsymbol{v}_v$ (cf. (6), (10) and (11)) of a quiescent single-component compressible particle-free fluid subject to a temperature gradient and undergoing pure heat conduction (so that $\boldsymbol{v}_m = \boldsymbol{0}$), with the said calculation having nothing whatsoever to do with either the issue of a no-slip boundary condition on a particle, or of the viability of Newton's law of viscosity. As regards the latter rheological issue, for a specified fluid, the calculation of the fluid's volume velocity $\boldsymbol{v}_v$ from (10), being independent of the fluid's rheological properties, does not depend upon whether the fluid is or is not Newtonian, much less the issue of whether the constitutive form of the fluid's deviatoric stress $\boldsymbol{T}$ derives from $\nabla\boldsymbol{v}_m$ or $\nabla\boldsymbol{v}_v$, were the fluid to prove to be Newtonian. Comparison of this theoretical $\boldsymbol{v}_v$ calculation with existing correlations of experimental data for the observed thermophoretic velocity $\boldsymbol{U}$ of non-heat-conducting particles in gases in the continuum region of Knudsen numbers revealed (Brenner 2005*b*) that $\boldsymbol{U}$ (which, remarkably, is found to be independent of particle size as well as of the particle's physical properties) and $\boldsymbol{v}_v$ were identical, at least to within the estimated uncertainty implicit in the correlation.

The preceding observation led to the seemingly inescapable conclusion that, despite the fact that the particle-free fluid was at rest ($\boldsymbol{v}_m = \boldsymbol{0}$), it was nevertheless already 'flowing' through space at a uniform velocity $\boldsymbol{v}_v$ prior to introducing the thermophoretic particle into the fluid. Hence, the obvious interpretation of the $\boldsymbol{U} = \boldsymbol{v}_v$ equality is that, when inserted into the fluid, the particle is subsequently entrained in this already flowing fluid, and is thus simply carried along passively therein. Given the notion that the fluid's Lagrangian velocity $\boldsymbol{v}_l$ has to be measured experimentally by monitoring the velocity of an inert and passive 'tracer' particle (Brenner 2005*b*) as it moves along the fluid's spatio-temporal trajectory, it seemed inevitable to thus identify the particle-free fluid's Lagrangian velocity $\boldsymbol{v}_l$ as being $\boldsymbol{v}_v$, rather than $\boldsymbol{v}_m$. Bear in mind that this purely kinematical conclusion has nothing whatsoever to do with whether it is $\boldsymbol{v}_m$ or $\boldsymbol{v}_v$ that appears in the constitutive form of Newton's law of viscosity for the particle-free fluid, or with whether the no-slip boundary condition on a particle in that fluid is imposed upon $\boldsymbol{v}_m$ or $\boldsymbol{v}_v$. Nor is our tracer-based conclusion that $\boldsymbol{v}_l = \boldsymbol{v}_v$ rooted in any fact stemming from Maxwell's (1879) thermal creep boundary condition imposed upon $\boldsymbol{v}_m$ at solid surfaces, nor from Maxwell's (1879) and Burnett's (1935, 1936) notions of the existence of thermal stresses in single-component quiescent gases (Kogan 1973, 1986, 2003; Kogan *et al.* 1976).

(In the preceding paragraph we have deliberately used the word 'flowing', rather than 'moving', in the same sense as one refers to heat 'flowing' by conduction through a fluid despite the absence of convective mass movement of the fluid. Heat or, more properly, energy share the common attribute of being abstract non-material extensive physical properties that can be transported solely by diffusion, rather than being carried through space in the company of mass. Volume is just another such non-material property.)

Given the above argument regarding the Lagrangian velocity of the fluid, it was natural to assume, subject to experimental verification, that the appropriate fluid-mechanical velocity $\boldsymbol{v}$ appearing in Newton's viscosity law as well as in the no-slip condition at solid surfaces should be the physically identifiable Lagrangian velocity of the fluid, namely $\boldsymbol{v}_l \equiv \boldsymbol{v}_v$. This point of view was pursued by Brenner & Bielenberg (2005), who used this pair of assumptions in place of their more conventional $\boldsymbol{v}_m$-based counterparts to solve theoretically the trio of continuity, linear momentum and energy equations for the thermophoretic velocity of a force- and torque-free small heat-conducting spherical particle through a Newtonian fluid, gaseous or liquid. That calculation led to results which agreed well with gaseous experimental thermophoretic data for the now heat-conducting particle case, again to within reasonable estimates of experimental uncertainties, thereby buttressing support for the correctness of the view that $\boldsymbol{v}_v$ rather than $\boldsymbol{v}_m$ should be used in Newton's viscosity law and in the no-slip boundary condition. The present paper was thus designed to show, by now solving this trio of theoretical equations for the case of gaseous thermal transpiration in capillaries, that this same pair of $\boldsymbol{v}_m \rightarrow \boldsymbol{v}_v$ changes also furnishes results that accord with experiment.

Strictly speaking, our several theoretical analyses, involving the respective solutions of this trio of equations (albeit species mass rather than energy in the two-component diffusiophoretic case), provide support for only our no-slip hypothesis, leaving unresolved the issue of whether Newton's law of viscosity should be based upon $\boldsymbol{v}_m$ or $\boldsymbol{v}_v$. The same is true of our present thermophoretic analysis. The because the distinction between the respective $\nabla \boldsymbol{v}_m$ and $\nabla \boldsymbol{v}_v$ viscosity contributions disappears from the linear momentum equation in both the thermophoretic (Brenner & Bielenberg 2005) and present thermal transpiration cases owing to the fact that $\mu_o \nabla^2 \boldsymbol{v}_v = \mu_o \nabla^2 \boldsymbol{v}_m$ in both, at least to terms of dominant order in the respective perturbation parameters. As such, the agreement of each of these analyses with data provides experimental evidence only for the viability of our no-slip hypothesis. However, as discussed in Brenner (2005*b*, §4), there does exist strong theoretical evidence for the viability of our Newton's law $\boldsymbol{v}_v$ hypothesis, such testimony being based upon its agreement with Burnett's (1935) extension of the Chapman–Enskog perturbation solution (Chapman & Cowling 1970) of Boltzmann's gas–kinetic theory equation, as embodied in Kogan's view of thermal stresses being on a par with

Newton's $\boldsymbol{v}_m$-based viscous stresses, and thus representing a distinct additional mechanism for the diffuse transport of momentum.

The molecular mechanism underlying the origin of these thermal stresses can be understood by recognizing the important distinction between mass and matter when focusing on an MFP in the case of single-component fluids within which temperature gradients exist, since each molecule (of mass m and velocity $\boldsymbol{u}$) carries with it an amount of momentum $m\boldsymbol{u}$ and energy $mu^2/2$. Because the individual velocities $\boldsymbol{u}$ are statistically distributed – and thus dependent, on average, upon the local temperature $T$of the fluid – it becomes theoretically possible in a single-component fluid for the mutual interchange of a pair of molecules initially lying on opposite sides of the MFP's surface to result in a net exchange of momentum and energy despite the fact that there is no net exchange of total mass. The existence of temperature gradients thus affords the possibility for a diffuse (i.e. non-convective) transport of momentum and energy across the MFP's material surface, above and beyond the standard amounts of these extensive properties associated with Newton's and Fourier's laws, respectively constituting diffuse momentum and energy transport processes. Were we to consider the case of, say, pure heat conduction in a fluid at rest, for which $\boldsymbol{v}_m = \boldsymbol{0}$, the traditional form of Newton's viscosity law, wherein $\boldsymbol{v} = \boldsymbol{v}_m$, would predict the absence of any diffuse viscous momentum transport. However, the existence of thermal stresses in gases in circumstances where $\boldsymbol{v}_m = \boldsymbol{0}$ has long been recognized, ever since the time of Maxwell (1879), as later confirmed by Burnett (1935, 1936). Such stresses arise in fluids for much the same reason as thermoelastic stresses arise in solids (Iesan & Scalia 1996; Noda, Hetnarski & Tanigawa 2002), namely, the non-uniform expansion of matter arising from density gradients, such gradients emanating from the dependence of the material's specific volume on temperature. While thermal stresses in gases are often assumed on the basis of Burnett's (1935, 1936) calculations to be non-continuum in nature, thus presumably arising only at non-zero Knudsen numbers, the work of Kogan and his collaborators (Kogan 1973, 1986, 2003; Kogan *et al.* 1976) negates this commonly held view. Explicitly, their work points out that during flow processes (i.e. $\boldsymbol{v}_m \neq \boldsymbol{0}$), when the Reynolds number characterizing the gas's motion is of order unity, the diffuse transport of momentum arising from thermal stresses is of the same order of magnitude as the diffuse transport of momentum arising from Newton's $\boldsymbol{v}_m$-based viscosity law. This issue is discussed at length by Brenner (2005*b*), where it is shown that the proposed replacement of $\boldsymbol{v}_m$ by $\boldsymbol{v}_v$ in Newton's viscosity law is, in the case of gases, exactly equivalent to the addition of these diffuse thermal stresses to Newton's traditional $\boldsymbol{v}_m$-based viscosity law, at least in the case of Maxwell molecules.

In summary, purely kinematical tracer velocity experiments based upon data in fluids from which solid surfaces are absent supports the view that a fluid's Lagrangian velocity is equal to its volume velocity rather than its mass velocity. Independently of this fact, experimentally based dynamical/energetic evidence, derived from the respective solutions of several viscous flow boundary-value problems, following comparison of their predictions with experimental data, supports the view that the no-slip boundary condition at solid surfaces should be imposed upon the volume- rather than mass-velocity. As yet, only purely theoretical arguments, derived from the kinetic theory of gases, exist in favour of our hypothesis that the velocity appearing in Newton's law of viscosity should be the volume velocity, although our hypothesis is, *ipso facto*, consistent with the same experimental data as currently supports belief in its present $\boldsymbol{v}_m$-based status. Another major question still outstanding (Brenner 2005*b*) is that of whether the constitutive equation for the specific momentum density of a fluid is given by $\boldsymbol{v}_m$, as is currently supposed, or, seemingly more rationally based upon its Lagrangian antecedents, by $\boldsymbol{v}_v$. Again, this issue can only be decided on the basis of experiment. All experiments to date fall within the range of creeping-flow Reynolds numbers, where contributions arising from inertial momentum effects are negligible relative to viscous effects.

6.4. *Concluding remarks*

From the comparisons presented in table 1, as well as those outlined in other publications (Bielenberg & Brenner 2005*b*; Brenner & Bielenberg 2005) concerned with our volume–velocity-based interpretation of thermophoretic and diffusiophoretic data, it is clear that this unconventional continuum-hydrodynamic theory (including the volume–velocity-based tangential no-slip boundary condition) outlined previously (Brenner 2005*b*), is consistent with a wide variety of experimental observations in gases, whose outcome has heretofore been explained as arising from Maxwell (1879) thermal creep slip effects. The latter slip is quantified in the literature by use of empirical phenomenological parameters or estimates thereof based upon the choice of an accommodation coefficient characterizing the nature of the gas–solid interaction, i.e. diffuse or back reflection of the gas molecules from the surface (Sharipov 2004), as was discussed earlier. In contrast, in our modified theory, the physicochemical nature of the solid surface is irrelevant to the phenomenon, a conclusion consistent with the available thermal transpiration data of Los & Fergusson (1952) as well as with related thermophoretic particle velocity correlations (Brenner & Bielenberg 2005), whose current interpretation also embodies the notion of Maxwell thermal creep. Our generic volume–velocity-based fluid-mechanical theory (Brenner 2005*b*) presumably applies equally to liquid-phase systems, having been put to the test in the case of interpreting thermal diffusion experiments (Bielenberg & Brenner 2005*a*). However, to the best of our knowledge, no thermal transpiration experiments involving liquids have yet been performed. Such notions for liquids, if correct, may prove to be of value in microfluidic and related applications (Braun & Libchaber 2002; Day 2003).

J.R.B. was supported by an NSF Graduate Fellowship. H.B. thanks Dr Sangtae Kim, formally of Eli Lilly and Company, for arranging funding of the present study by that organization.

REFERENCES

Alexandrov, V. Yu, Friedlander, O. G & Nikolsky, Yu. V. 2003 Numerical and experimental investigations of thermal stress effect on nonlinear thermomolecular pressure difference. In *Rarefied Gas Dynamics: 23rd International Symp.* (ed. A. D. Ketsdever & E. P. Muntz), pp. 250–257. Am. Inst. Phys.

Annis, B. K. 1972 Thermal creep in gases. *J. Chem. Phys.* **57**, 2898–2905.

Bielenberg, J. R. & Brenner, H. 2005*a* A hydrodynamic/Brownian motion model of thermal diffusion in liquids. *Physica* A **356**, 279–293.

Bielenberg, J. R. & Brenner, H. 2005*b* A continuum approach to phoretic motions: diffusiophoresis. *Phys. Fluids* (in press).

Bird, R. B., Stewart, W. E. & Lightfoot, E. N. 2002 *Transport Phenomena*, 2nd edn. Wiley.

Bobylev, A. V. 1995 Quasistationary hydrodynamics for the Boltzmann equation. *J. Stat. Phys.* **80**, 1063–1083.

Braun, D. & Libchaber, A. 2002 Trapping of DNA by thermophoretic depletion and convection. *Phys. Rev. Lett.* **89**, 188103-1 to 4.

Brenner, H. 2004 Is the tracer velocity of a fluid continuum equal to its mass velocity? *Phys. Rev.* E. **70**, 061201-1 to 10.

Brenner, H. 2005*a* Kinematics of volume transport. *Physica* A **349**, 11–59.

Brenner, H. 2005*b* Navier–Stokes revisited. *Physica* A **349**, 60–132.

Brenner, H. & Bielenberg, J. R. 2005 A continuum approach to phoretic motions: thermophoresis. *Physica* A **355**, 251–273.

Brush, S. G. 1976 *The Kind of Motion that we call Heat*. North-Holland.

Burnett, D. 1935 The distribution of velocities in a slightly non-uniform gas. *Proc. Lond. Math. Soc.* **39**, 385–430.

Burnett, D. 1936 The distribution of molecular velocities and mean motion in a non-uniform gas. *Proc. Lond. Math. Soc.* **40**, 382–435.

Chapman, S. & Cowling, T. G. 1970 *Mathematical Theory of Non-uniform Gases*, 3rd edn. Cambridge University Press.

Crookes, W. 1876 On repulsion resulting from radiation. Parts III and IV. *Phil. Trans. R. Soc. Lond.* **166**, 325–376.

Day, C. 2003 Thermal gradients can boost the local concentration of DNA in solution. *Phys. Today* **56**, 16–17.

Derjaguin, B. V. & Yalamov, Yu. 1965 Theory of thermophoresis of large aerosol particles. *J. Colloid Sci.* **20**, 555–570.

Derjaguin, B. V. & Yalamov, Yu. I. 1972 The theory of thermophoresis and diffusiophoresis of aerosol particles and their experimental testing. In *Topics in Current Aerosol Research* (*Part 2*) (ed. G. Hidy & J. Brock), pp. 1–200. Pergamon.

Derjaguin, B. V., Rabinnovich, Ya. I., Storozhilova, A. I. & Shcherbina, G. I. 1976 Measurement of the coefficient of thermal slip of gases and the thermophoretic velocity of large-size aerosol particles. *J. Colloid Interface Sci.* **57**, 451–461.

De Groot, S. R. & Mazur, P. 1984 *Non-equilibrium Thermodynamics*, 2nd edn. Dover.

Hirschfelder, J. O., Curtiss, C. F. & Bird, R. B. 1954 *Molecular Theory of Gases and Liquids*. Wiley.

Iesan, D. & Scalia, A. 1996 *Thermoelastic Deformations*. Kluwer.

Knudsen, M. 1910 Thermischer Molekulardruck der Gase in Röhren. *Annln Phys.* (Leipzig) **33**, 1435–1448.

Kogan, M. N. 1973 Molecular gas dynamics. *Annu. Rev. Fluid Mech.* **5**, 383–405.

Kogan, M. N. 1986 Non-Navier–Stokes gas dynamics and thermal stress phenomena. In *Proc. 15th Intl Symp. Rarefied Gas Dynamics* (ed. V. Boffi, C. Cercignani & B. G. Tuebner), vol. 1, pp. 15–24.

Kogan, M. N. 2003 Some solved and unsolved problems in kinetic theory. In *Rarefied Gas Dynamics: 23rd Intl Symp.* (ed. A. D. Ketsdever & E. P. Muntz), pp. 1–9. *Am. Inst. Phys.*

Kogan, M. N., Galkin, V. S. & Friedlander, O. G. 1976 Stresses arising in gases due to temperature and concentration inhomogeneities. New types of free convection. *Sov. Phys. Ups.* **19**, 420–438.

Lauga, E., Brenner, M. P. & Stone, H. A. 2005 Microfluidics: the no-slip boundary condition. In *Handbook of Experimental Fluid Dynamics* (ed. J. Foss, C. Tropea & A. Yarin), chap. 15. Springer.

Los, J. M. & Fergusson, R. R. 1952 Measurements of thermomolecular pressure differences in argon and nitrogen. *Trans. Faraday Soc.* **48**, 730–738.

Maxwell, J. C. 1879 On stresses in rarified gases arising from inequalities of temperature. *Phil. Trans. R. Soc.* A **170**, 231–262.

Noda, N., Hetnarski, R. B. & Tanigawa, Y. 2002 *Thermal Stresses*. Taylor & Francis.

Papadopoulos, D. H. & Rosner, D. E. 1995 Enclosure gas flows driven by non-isothermal walls. *Phys. Fluids* **7**, 2535–2537.

Passian, A., Warmak, R. J., Ferrell, T. L. & Thundat, T. 2003 Thermal transpiration at the microscale: a Crookes' cantilever. *Phys. Rev. Lett.* **90**, 124503-1 to 4.

Reynolds, O. 1879 On certain dimensional properties of matter in the gaseous state. Part I. Experimental researches on thermal transpiration of gases through porous plates and on the laws of transpiration and impulsion, including an experimental proof that gas is not a continuous plenum. Part II. On an extension of the dynamical theory of gas, which includes the stresses, tangential and normal, caused by a varying condition of gas, and affords an explanation of the phenomena of transpiration and impulsion. *Phil. Trans. R. Soc.* B **170**, 727–845.

Rosner, D. E. 1989 Side-wall gas 'creep' and 'thermal stress convection' in microgravity experiments on film growth by vapor transport. *Phys. Fluids* A **1**, 1761–1763.

Rosner, D. E. & Papadopoulos, D. H. 1996 Jump, slip, and creep boundary conditions at non-equilibrium gas/solid interfaces. *Ind. Engng Chem. Res.* **35**, 3210–3222.

Sharipov, F. 2004 Heat transfer in the Knudsen layer. *Phys. Rev.* E **69**, 061201-1 to 4.

Slattery, J. C. 1972 *Momentum, Energy, and Mass Transfer in Continua.* McGraw–Hill.

Talbot, L., Cheng, R. K., Schefer, R. W. & Willis, D. 1980 Thermophoresis of particles in a heated boundary layer. *J. Fluid. Mech.* **101**, 737–758.

Van Dyke, M. 1975 *Perturbation Methods in Fluid Mechanics*, 2nd. edn. Parabolic.

Waldmann, L. & Schmitt, K. 1966 Thermophoresis and diffusiophoresis of aerosols. In *Aerosol Science* (ed. C. N. Davies), pp. 137–162. Academic.